Heat transport in $Sb_{2-x}V_xTe_3$ single crystals

J. S. Dyck,* W. Chen, and C. Uher
Department of Physics, University of Michigan, Ann Arbor, Michigan 48109

Č. Drašar and P. Lošťák
Faculty of Chemical Technology, University of Pardubice, Čs. Legií 565, 532 10 Pardubice, Czech Republic
(Received 12 April 2002; revised manuscript received 28 June 2002; published 24 September 2002)

Antimony telluride doped with small concentrations of vanadium was recently identified as a diluted magnetic semiconductor. We present a study of the heat transport in single crystals of $Sb_{2-x}V_xTe_3$ with $x=0$, 0.01, 0.02, and 0.03. Thermopower and thermal conductivity were measured from 1.5 K to 300 K. The thermopower is positive for all samples investigated and has a modest dependence on vanadium content. At low temperatures, the lattice thermal conductivity has an approximate T^2 dependence and the data up to 100 K can be fitted well assuming that phonons scatter on boundaries, point defects, charge carriers, and other phonons. Theoretical analysis reveals that the over-riding effect of vanadium impurity is the formation of point defects that suppress heat transport via both mass and elastic strain fluctuations.

DOI: 10.1103/PhysRevB.66.125206 PACS number(s): 75.50.Pp, 66.70.+f, 63.20.Kr

I. INTRODUCTION

Antimony telluride Sb_2Te_3 is a narrow-gap semiconductor that belongs to the group of tetradymite-type layered compounds having the formula $A_2^{V}B_3^{VI}$ (with $A=$ Sb, Bi and $B=$ Se, Te). Crystals in this family are composed of repeated planes of five-atomic layer lamellas separated by a van der Waals gap. This unusual structure results in highly anisotropic transport properties. Alloys of these binary compounds have excellent room temperature thermoelectric properties and have served as the backbone of the thermoelectric cooling technology. As such, their electrical and thermal transport properties have been thoroughly studied.

In the case of pure Sb_2Te_3, however, most of the studies have been focused on electrical, optical, and galvanomagnetic behavior. The bulk of the thermal conductivity investigations in the literature are focused on the room temperature behavior of the Sb_2Te_3-Bi_2Te_3 alloys. Data on the temperature dependence of the thermal conductivity of Sb_2Te_3 are limited and only extend down to 80–100 K.[1–4] The high native concentration of holes ($\sim 10^{20}$ cm^{-3}) in nominally undoped Sb_2Te_3 makes a significant contribution to the heat transport and is, in fact, the dominant effect near room temperature.[5]

The doping influence of a great number of foreign impurites in Sb_2Te_3 has been studied.[5–9] Very recently, we found that Sb_2Te_3 becomes a ferromagnetic semiconductor at low temperatures upon addition of small concentrations of vanadium.[10] The Curie temperature increases with vanadium content and reaches approximately 22 K for $Sb_{1.97}V_{0.03}Te_3$. Furthermore, the presence of the magnetic ion has a strong influence on the electrical transport properties near the Curie temperature. So far there has been no report of heat transport in this material. In this work, we present thermal conductivity and thermoelectric power data from 1.5 to 300 K for single crystals of $Sb_{2-x}V_xTe_3$, and we analyze the influence of vanadium.

II. EXPERIMENTAL TECHNIQUES

The synthesis of single crystals of $Sb_{2-x}V_xTe_3$ with $x=0$, 0.01, 0.02, 0.03 (nominal) using a modified Bridgeman technique and a description of their electronic and magnetic properties is described elsewhere.[10] Measurement of thermal conductivity κ and thermopower S perpendicular to the c axis was carried out in a cryostat equipped with two radiation shields employing a longitudinal steady-state technique. Samples with typical dimension $3\times3\times10$ mm^3, where the direction of the long dimension is in the c plane were cut using a spark erosion machine. For sample temperatures of 5–300 K, thermal gradients were measured with the aid of fine copper-constantan thermocouples. The copper legs of the thermocouples served as Seebeck voltage probes and the sample thermopower was corrected for the contribution of the previously calibrated Cu wires. The temperature range of 1.5–25 K was covered in separate experiments employing Ge thermometers to measure thermal gradients. A miniature strain gauge served as a heat source in both cases. Thermal conductivity data were experimentally corrected for radiation loss.[11] The magnitude of this correction was approximately 8–9 % at room temperature and <1% at 100 K.

III. RESULTS AND DISCUSSION

The temperature dependence of the thermopower is displayed in Fig. 1. All samples have positive thermopower indicating hole transport, which is consistent with positive Hall coefficients for these samples.[10] The Fermi surface of the Sb_2Te_3 valence band is generally described by a six-ellipsoidal model[12] and the behavior of the thermopower and other transport properties have been interpreted by assuming the presence of an upper as well as a lower valence band[3,7,13] or by considering a single band with anisotropic, mixed carrier relaxation times.[14,15] The room temperature value of 89 μV/K for our pure Sb_2Te_3 sample compares favorably to the existing data in the literature for a comparably doped material.[16] Here, we wish to highlight the effect of vana-

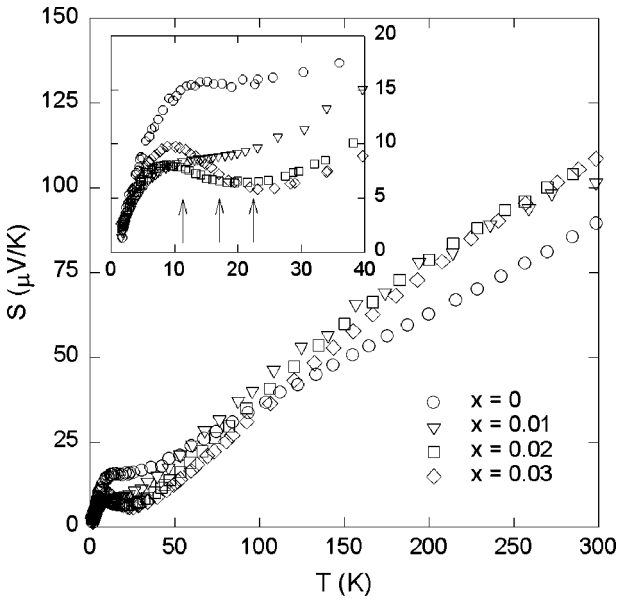

FIG. 1. Temperature dependence of the thermopower (S) for $Sb_{2-x}V_xTe_3$ single crystals. The inset is an expanded view at low temperatures. The arrows correspond to the Curie temperatures which are 11 K, 17 K, and 22 K for $x = 0.01$, 0.02, and 0.03, respectively.

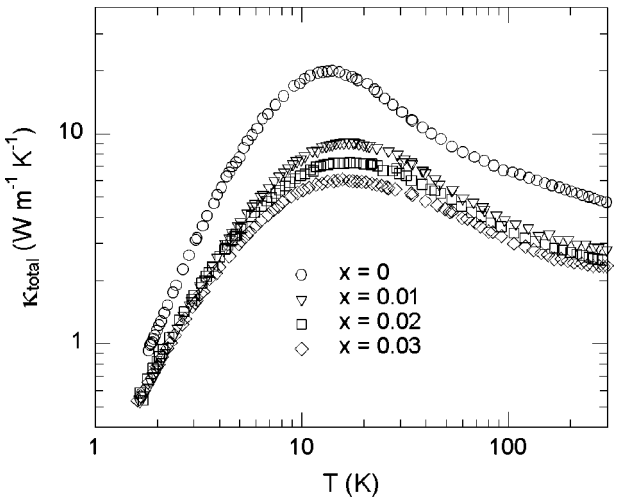

FIG. 2. Temperature dependence of the total thermal conductivity (κ) for $Sb_{2-x}V_xTe_3$ single crystals.

dium. The room temperature thermopower S increases with the addition of vanadium to a value of approximately 110 μV/K for $x=0.02$ and 0.03. We note that over the same range of x, the electrical conductivity σ decreases by a factor of 5, and the Hall coefficient remains approximately constant. A relative insensitivity of S to the value of conductivity has been observed for a number of different dopants in Sb_2Te_3 and has been explained by invoking a two-band model,[7] or alternatively by the interaction of the incorporated foreign atom with native (antisite and vacancies) point defects.[17]

At low temperatures, shown in the inset of Fig. 1, diffusive as well as phonon drag effects are present. A large phonon drag peak is seen for pure Sb_2Te_3. A similar feature is also present in vanadium-doped samples, though with reduced magnitude and the peak shifted to lower temperatures. It is in this temperature regime that both the resistivity and the Hall coefficient have a maximum associated with the transition to the magnetically ordered state. Interestingly, S is suppressed rather than enhanced and the minimum in S occurs very close to the Curie temperature of each respective sample (denoted by arrows in the inset for Fig. 1). These observations suggest a modification of the electron-phonon interaction (phonon drag) or the density of states due to the presence of vanadium ions. A detailed magneto-thermopower study would further elucidate this behavior.

The temperature dependence of the total thermal conductivity is given in Fig. 2. $\kappa(T)$ for Sb_2Te_3 increases as temperature decreases and develops a peak at a temperature near 13 K. Below the peak, κ decreases with an approximate T^2 dependence. As vanadium is incorporated into the structure, κ is suppressed at all temperatures with the largest reduction near the peak. Thermal conductivity, in general, is the sum of two components; i.e., $\kappa=\kappa_e+\kappa_L$ where κ_e and κ_L are the electronic and lattice thermal conductivity contributions, respectively. From the results of Ref. 10, the electrical conductivity decreases with x. Thus, at least part of the suppression in κ is due to a decrease in κ_e which is determined using the Wiedemann-Franz ratio, $\kappa_e=L\sigma T$ where L is the Lorenz number and T is the absolute temperature.

The exact calculation of κ_e is complicated by the likely presence of two valence bands, the parameters of which are not well established. L is dependent on reduced Fermi level and scattering mechanism, and can be temperature dependent for semiconductors. Following the formalism of Fistul,[18] if we allow for a mixed scattering on acoustic phonons and ionized impurities, and utilize thermopower and Hall coefficient data, we find that at room temperature, L is in the range $(1.9–2.3)\times10^{-8}$ V^2/K^2 depending on the chosen relative strength of the scattering mechanisms (the lower bound corresponding to scattering dominated by acoustic phonons and the upper bound corresponding to scattering on impurities). Impurity scattering will become more important as temperature is decreased, and we argue that L should tend to the elastic limit; i.e., $L=2.44\times10^{-8}$ V^2/K^2. Stordeur and Simon[14] reported that the Lorenz number increased from approximately 2.1×10^{-8} at 300 K to 2.4×10^{-8} V^2/K^2 at 100 K in Sb_2Te_3 single crystals. Pure and doped antimony tellurides have a large electronic contribution to the room temperature thermal conductivity. In the case of complete degeneracy, the magnitude of κ_e at room temperature for the undoped material is up to 70 % of the total thermal conductivity, and $\sim$40% for $Sb_{1.97}V_{0.03}Te_3$. However, the proportion decreases as temperature decreases; furthermore, the error made in the determination of κ_L from an uncertainty in $\kappa-\kappa_e$ is correspondingly diminished at lower temperatures as well. Therefore, we approximate L to be 2.44×10^{-8} V^2/K^2 independent of temperature, and restrict our theoretical analysis of κ_L to temperatures from 1.5–100 K. The uncertainty in κ_L due to the uncertainty in κ_e is $\sim$7% for $x=0$ and $\sim$1% for $x=0.03$ at 100 K and $<$1% below 50 K for all samples. Using this approach, i.e., limiting the

analysis to temperatures below 100 K, we essentially assure that the temperature dependence of the lattice thermal conductivity is insensitive to the model chosen for the electronic contribution.

The temperature dependence of lattice thermal conductivity is normally treated within the Debye approximation. We performed theoretical fits of the lattice thermal conductivity for all $Sb_{2-x}V_xTe_3$ samples using the following expression:[19]

$$\kappa_L(T)=\frac{k_B}{2\pi^2\nu}\left(\frac{k_BT}{\hbar}\right)^3\int_0^{\theta_D/T}\tau_c\frac{y^4e^y}{(e^y-1)^2}dy, \qquad (1)$$

where ω is the phonon frequency, k_B is the Boltzmann constant, $\hbar$ is the reduced Planck constant, y stands for the dimensionless parameter $y=\hbar\omega/k_BT$, θ_D is the Debye temperature, ν is the velocity of sound, and τ_c is the phonon-scattering relaxation time. The combined phonon-scattering relaxation rate τ_c^{-1} can be written as

$$\tau_c^{-1}=\frac{\nu}{d}+A\omega^4+B\omega^2T\exp\left(-\frac{\theta_D}{3T}\right)+C\omega, \qquad (2)$$

where d is the crystal size and the coefficients A, B, and C are independent of temperature. The terms in Eq. (2) represent boundary scattering, point-defect (Rayleigh) scattering, three-phonon umklapp scattering, and carrier-phonon scattering, respectively. The first three terms are physically essential to account for the extrinsic and intrinsic phonon-scattering processes in real dielectric crystals. Ziman[20] derived the inverse phonon relaxation time τ_{e-p}^{-1} for scattering by free carriers in a parabolic band. For metals or degenerate semiconductors it takes the form of the fourth term in Eq. (2) provided $\ell_h \gg \lambda_{ph}$ where ℓ_h is the mean-free path of charge carriers (holes in this case) and λ_{ph} is the phonon wavelength. For $\ell_h \ll \lambda_{ph}$, the theory underlying this result breaks down[21] and τ_{e-p}^{-1} becomes proportional to ω^2 rather than ω^1. In Fig. 3, we show a comparison of ℓ_h and λ_{ph} calculated using formal Drude analysis of the electrical transport data and the dominant phonon method ($h\nu/\lambda_{ph} \sim 2k_BT$) for the $Sb_{2-x}V_xTe_3$ series. This illustrates that the form in Eq. (2) is appropriate for Sb_2Te_3, but may become borderline for the vanadium-doped samples at low temperatures.

Theoretical fits of the temperature dependence of the lattice thermal conductivity of $Sb_{2-x}V_xTe_3$ from 1.5–100 K to Eqs. (1) and (2) are compared to the data in Fig. 4. The smallest dimension of each single crystal was used for the parameter d and the prefactors A, B, and C were fitting parameters. The Debye temperature of Sb_2Te_3 is reported[22] to be 160 K at 80 K. It is worth noting that θ_D of both Bi_2Te_3 and Bi_2Se_3 has a strong temperature dependence below 80 K with a minimum[23] near 10 K. We expect θ_D of Sb_2Te_3 to have a similar temperature dependence. Good fits were obtained using the temperature-dependent Debye temperature data of Bi_2Te_3 [$\theta_D(T)$] from Ref. 22 which has a value of 162 K at 80 K. Nominally better fits were obtained using $\theta_D(T)/n^{1/3}$ with $n=5$ following the prescription of Roufosse and Klemens[24] for crystals made up of molecular groups of n atoms. Only minor quantitative differences in the fitting parameters resulted between the two schemes, and the fits shown correspond to the latter one. To our knowledge, no value for the speed of sound in Sb_2Te_3 exists in the literature. We obtain an estimate of $\nu=2900$ m/s from fitting the specific heat data of Zhdanov[25] to Debye theory and this value is used in our fitting procedure.

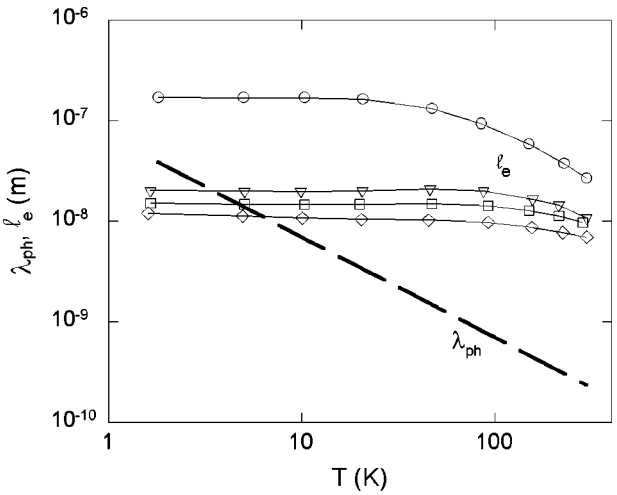

FIG. 3. Estimated hole mean-free path (ℓ_h) and phonon wavelength (λ_{ph}) as a function of temperature for the $Sb_{2-x}V_xTe_3$ series determined using formal Drude analysis for ℓ_h and the dominant phonon method for λ_{ph}. Symbol definitions are the same as for Figs. 1 and 2.

The results of the theoretical analysis are given in Table I. As an aside, we also found that the data can be nicely fit without taking into account carrier-phonon interaction provided the grain size is allowed to decrease to very small

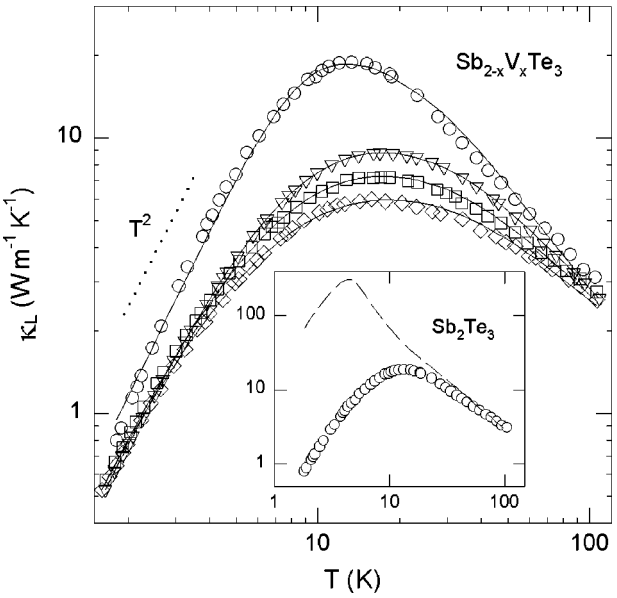

FIG. 4. Temperature dependence of the lattice thermal conductivity (κ_L) for $Sb_{2-x}V_xTe_3$ single crystals. The solid lines through the data are theoretical fits to Eqs. (1) and (2). Fitting parameters are found in Table I. The inset displays the same model calculation (dashed line) without electron-phonon interaction compared to the data for pure Sb_2Te_3.

TABLE I. Fitting parameters for the theoretical analysis of the lattice thermal conductivity of $Sb_{2-x}V_xTe_3$ single crystals. See text for details.

x	$A(10^{-43}\ s^3)$	$B(10^{-18}$ s/K)	$C(10^{-4})$
0	0.97	12.52	1.02
0.01	37.39	10.24	1.48
0.02	70.88	9.46	1.36
0.03	119.35	8.33	1.34

dimensions of $\sim 30\ \mu$m. This micron-size length scale does not correspond to any characteristic physical feature in these single crystals (it is two orders of magnitude smaller than the physical size of the single crystalline specimen and four orders of magnitude larger than the spacing between five-layer lamellas forming the tetradymite structure). We thus consider such a result as unacceptable. Fixing the boundary scattering parameter at the smallest crystal dimension and considering only boundary, point defect, and umklapp scattering, we obtain in the case of pure Sb_2Te_3 the dashed curve in the inset to Fig. 4. In order to bring the theory and data into agreement while using the actual smallest crystal dimension (2 mm) for the boundary scattering parameter d, it is essential to incorporate the carrier-phonon scattering term in the fitting routine.

The prefactor for the carrier-phonon scattering inverse relaxation time is[26]

$$C=\frac{(\epsilon_1 m^*)^2}{2\pi\hbar^3\rho\nu}, \tag{3}$$

where ϵ_1 is the deformation potential, m^* is the hole effective mass, and ρ is the mass density. To our knowledge, ϵ_1 for Sb_2Te_3 is so far unknown. With $\rho=6.5$ g/cm^3 and $m^* \simeq 0.25m_0$ (m_0 is the electron mass), the fitted value of C implies that ϵ_1 is ≈ 3 eV, which seems quite reasonable. Upon addition of vanadium to the structure, the value of C increases somewhat in comparison to that of pure Sb_2Te_3, but no clear trend is seen as a function of the actual vanadium concentration. An enhancement of the effective mass could be responsible for this trend. According to the calculations shown in Fig. 3, the criterion that $\ell_h \gg \ell_{ph}$ may not be satisfied below 10 K where the effect of the carrier-phonon interaction is most pronounced. κ_L should be proportional to T^2 in the temperature range where the carrier-phonon interaction dominates if τ_{e-p}^{-1} depends linearly on ω. On the other hand, if $\tau_{e-p}^{-1} \sim \omega^2$ as is the case when $\ell_h \ll \ell_{ph}$, then $\kappa_L \sim T$. Inspection of $\kappa_L(T)$ at low temperatures for the undoped sample reveals a clear T^2 dependence, while for the doped samples the temperature dependence is marginally weaker but may be asymptotically approaching T^2 also. Perhaps, it is not surprising that an offset in C is seen in the doped samples, given we are in a regime where $\ell_h \sim \ell_{ph}$. It is also possible that the incorporation of vanadium into the crystal lattice gives rise to formation of line defects that mimic the frequency dependence of the scattering rate of τ_{e-p}^{-1} and by neglecting the presence of these line defects we see artificially enhanced values of the parameter C.

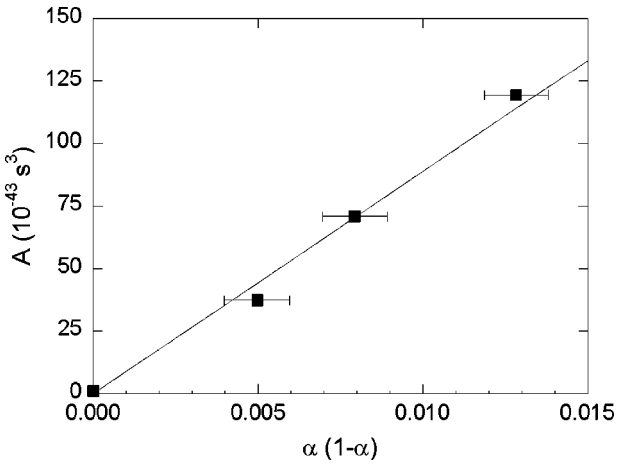

FIG. 5. Point defect prefactor term (A) versus vanadium content $[\alpha(1-\alpha)]$ for $Sb_{2-x}V_xTe_3$. See text for details. Error bars are estimated from the uncertainty in the determination of $x=2\alpha$.

Upon inspecting the fitting parameters in Table I, it is clear that the primary influence of vanadium on the lattice thermal conductivity of Sb_2Te_3 arises via the large variation in the point defect scattering prefactor A, which can be written,[27]

$$A=\frac{\Omega_0\Gamma}{4\pi\nu^3}, \tag{4}$$

where Ω_0 is the unit cell volume and Γ is the scattering parameter appropriate for a substitutional impurity in Sb_2Te_3. For a single lattice site, taking into account both mass fluctuation and strain field scattering,[28]

$$\Gamma=\alpha(1-\alpha)[(\Delta M/M_{ave})^2+\epsilon(\Delta\delta/\delta_{ave})^2], \tag{5}$$

where α is the relative concentration of the impurity on that lattice site, $\Delta M=M_i-M$ is the mass difference between an impurity and the atom normally associated with that lattice site, $\Delta\delta=\delta_i-\delta$ is the difference in ionic radii of the two species, M_{ave} and δ_{ave} are the weighted averages of the mass and the radius at this lattice site, respectively, and ϵ is a phenomenological parameter. For a compound A_aB_b, the composite Γ is

$$\Gamma(A_aB_b)=\frac{a}{a+b}\left(\frac{M_A}{M_m}\right)^2\Gamma(A)+\frac{b}{a+b}\left(\frac{M_B}{M_m}\right)^2\Gamma(B), \tag{6}$$

where $M_m=(aM_a+bM_b)/(a+b)$. Applying this to $Sb_{2-x}V_xTe_3$, we take A = (Sb,V) where V is the impurity substituting for Sb and B=Te. Magnetic and electrical transport properties[10] suggest that vanadium resides on the Sb sublattice and takes a trivalent V^{3+} state. Since there is no substitution on the Te sublattice, the second term in Eq. (6) is zero, and $\Gamma(Sb_2Te_3)=0.129\ \Gamma(Sb)$. The exact radii of Sb and V in $Sb_{2-x}V_xTe_3$ are not known. However, adopting a formal valence picture, the radii of Sb and V are 0.90 Å and 0.78 Å, respectively, yielding $\Delta\delta/\delta=-0.13$. Figure 5 plots

the fitted values of A versus $\alpha(1-\alpha)$ where $\alpha = x/2$ together with the predictions of Eqs. (4)–(6) with the above assumptions and with the fitted strain parameter $\epsilon = 235$. While this picture would adequately explain the data, the presence of other type point defects arising from the presence of vanadium (e.g., vacancies) could contribute to the overall value of A, and ϵ could be less than this value. Yokota and Katayama[4] obtained $\epsilon = 400$ for $(Bi_{1-x}Sb_x)_2Te_3$ alloys indicating that phonon scattering resulting from the change of atomic radius by substitution is stronger than that resulting from the change of atomic mass. Our analysis (and the value of $\epsilon = 235$) also suggests that atomic radius fluctuations, i.e., the elastic strain, likely plays an important role in the thermal transport.

The umklapp scattering term in Eq. (2) is a semiempirical expression that has been used successfully in the description of a variety of materials[29–31] and B is written

$$B = \frac{n^{2/3}\hbar\gamma^2}{M\theta_D\nu^2}, \tag{7}$$

where γ is the Grüneisen parameter and M is the average atomic mass. There appears a small decreasing trend in the fitted value of B (see Table I). A possible explanation is that the incorporation of vanadium stiffens the lattice, leading to an increase in both θ_D and ν. In fact, we believe that 3 at. % vanadium is near the upper solubility limit for the bulk growth of the compound—attempts to incorporate significantly larger quantities of vanadium result in the segregation of secondary phases. The relative importance of strain in the point defect scattering shown above is consistent with this picture.

As we noted, vanadium-doped Sb_2Te_3 develops a ferromagnetic order at low temperatures—Curie temperatures for $Sb_{2-x}V_xTe_3$ are 11 K, 17 K, and 22 K for $x = 0.01$, 0.02, and 0.03, respectively.[10] Thus, some discussions regarding the effect of resonant phonon scattering or magnon heat transport is in order. Low-temperature thermal conductivity is often sensitive to the presence of paramagnetic ions in insulating crystals. For example, resonant phonon scattering is observed in Al_2O_3 doped with small quantities of vanadium[32] due to transitions between low-lying energy levels of V^{4+}, while practically no effect is found from the presence of V^{3+}. The energy splittings due to the crystal fields and spin-orbit coupling are not known for vanadium in Sb_2Te_3. The orbital portion of the total angular momentum should be quenched because of the degenerate valence band, which should lead to a much smaller spin-orbit splitting than for Al_2O_3. The absence of any clear resonant dip in $\kappa_L(T)$ could imply that these energies lie outside (below) the temperature range explored. On the other hand, the scattering due to point defects and electron-phonon interaction is quite strong and could overwhelm any resonant scattering contribution. In any case, we see no obvious evidence in the thermal conductivity for resonant phonon scattering from the paramagnetic vanadium ion. Resonant phonon-magnon scattering might also be possible in $Sb_{2-x}V_xTe_3$. The phonon relaxation rate due to scattering of phonons by magnetic fluctuations[33] can be described by $\tau_{mag}^{-1} = D\omega^2/[(T-T_C)^q + G]$ which would lead to a local minimum or an inflection in κ_L near T_C. For temperatures below T_C, magnon heat transport can be expected to show a T^2 dependence in the thermal conductivity,[34] though this would be an enhancement relative to pure Sb_2Te_3 contrary to our observations. The data in Fig. 4 do not show these features, and so we concluded that magnetic properties have no clear effect on the zero-field thermal conductivity for temperatures down to 1.5 K.

IV. SUMMARY

Thermal transport properties of single crystals of $Sb_{2-x}V_xTe_3$ with $x = 0$, 0.01, 0.02, and 0.03 were measured. Thermopower increased modestly at room temperature with increasing vanadium concentration, while at low temperatures the vanadium tends to suppress the otherwise prominent phonon drag contribution. Near room temperature, the total thermal conductivity is dominated by charge carrier (hole) heat transport. Lattice thermal conductivity data below a temperature of 100 K are explained using the Debye model (with a temperature dependent Debye temperature) within the relaxation time approximation assuming scattering from crystal boundaries, carrier-phonon interaction, point defects, and three-phonon umklapp processes. The most notable effect of vanadium on the lattice thermal conductivity is the enhanced role of point defects. The influence arises not only from mass defect scattering, but also from the elastic strain associated with the different radii of antimony and vanadium. We observe no direct evidence of resonant phonon scattering due to low-lying energy levels of vanadium ions in the paramagnetic state, nor of a magnon contribution to the heat transport in the ferromagnetic state.

ACKNOWLEDGMENT

We wish to acknowledge the National Science Foundation International Programs grant between the University of Michigan and the University of Pardubice, Czech Republic.

*Email address: jdyck@umich.edu

[1] L. R. Testardi, J. N. Bierly, Jr., and F. J. Donahoe, J. Phys. Chem. Solids **32**, 1209 (1962).
[2] C. H. Champness, P. T. Chiang, and P. Parekh, Can. J. Phys. **43**, 653 (1964).
[3] I. A. Smirnov, A. A. Andreev, and V. A. Kutasov, Sov. Phys. Solid State **10**, 1403 (1968) [Fiz. Tverd. Tela **10**, 1782 (1968)].
[4] K. Yokota and S. Katayama, Jpn. J. Appl. Phys. **12**, 1205 (1973).
[5] P. Lostak, C. Drasar, A. Krejcova, L. Benes, J. S. Dyck, W. Chen, and C. Uher, J. Cryst. Growth **222**, 565 (2001).
[6] A. J. Rosenberg and A. J. Strauss, J. Phys. Chem. Solids **19**, 105 (1961).
[7] B. Rönnlund, O. Beckman, and H. Levy, J. Phys. Chem. Solids **26**, 1281 (1964).
[8] J. Horak, M. Matyas, and L. Tichy, Phys. Status Solidi A **27**, 621 (1975).

[9] V. A. Kulbachinskii, N. Miura, H. Nakagawa, C. Drasar, and P. Lostak, J. Phys.: Condens. Matter **11**, 5273 (1999).
[10] J. S. Dyck, P. Hajek, P. Lostak, and C. Uher, Phys. Rev. B **65**, 115212 (2002).
[11] J. S. Dyck, W. Chen, C. Uher, L. Chen, X. Tang, and T. Hirai, J. Appl. Phys. **91**, 3698 (2002).
[12] J. R. Drabble and R. Wolfe, Proc. Phys. Soc. London, Sect. B **69**, 1101 (1956).
[13] V. A. Kulbachinskii, Z. M. Dashevskii, M. Inoue, M. Sasaki, H. Negishi, W. X. Gao, P. Lostak, J. Horak, and A. de Visser, Phys. Rev. B **52**, 10 915 (1995).
[14] M. Stordeur and G. Simon, Phys. Status Solidi B **124**, 799 (1984).
[15] T. Caillat, L. Gailliard, H. Scherrer, and S. Scherrer, J. Phys. Chem. Solids **54**, 575 (1993).
[16] H. Scherrer and S. Scherrer, in *CRC Handbook of Thermoelectrics*, edited by D. M. Rowe (Chemical Rubber, Boca Raton, FL, 1995), pp. 211–237.
[17] T. Plechacek and J. Horak, J. Solid State Chem. **145**, 197 (1999).
[18] V. I. Fistul, *Heavily Doped Semiconductors* (Plenum, New York, 1969).
[19] J. Callaway, Phys. Rev. **113**, 1046 (1959).
[20] J. M. Ziman, *Electrons and Phonons* (Clarendon, Oxford, UK, 1960).
[21] A. B. Pippard, Philos. Mag. **46**, 1104 (1955).
[22] P. V. Gultyaev and A. V. Petrov, Sov. Phys. Solid State **1**, 330 (1959).
[23] G. E. Shoemake, J. A. Rayne, and R. W. Ure, Phys. Rev. **185**, 1046 (1969).
[24] M. Roufosse and P. G. Klemens, Phys. Rev. B **7**, 5379 (1973).
[25] V. M. Zhdanov, Russ. J. Phys. Chem. **45**, 1357 (1971).
[26] J. E. Parrott and A. D. Stuckes, *Thermal Conductivity of Solids* (Pion Limited, London, 1975), p. 68.
[27] P. G. Klemens, Proc. Phys. Soc. London **A68**, 1113 (1955).
[28] B. Abeles, Phys. Rev. **131**, 1906 (1963).
[29] G. A. Glassenbrenner and G. A. Slack, Phys. Rev. **134**, A1058 (1964).
[30] D. G. Onn, A. Witek, Y. Z. Qiu, T. R. Anthony, and W. F. Banholzer, Phys. Rev. Lett. **68**, 2806 (1992).
[31] D. T. Morelli, T. Caillat, J.-P. Fleurial, A. Borshchevsky, J. Vandersande, B. Chen, and C. Uher, Phys. Rev. B **51**, 9622 (1995).
[32] A. M. de Goër and N. Devismes, J. Phys. Chem. Solids **33**, 1785 (1972).
[33] G. S. Dixon and D. Walton, Phys. Rev. **188**, 735 (1969).
[34] H. Sato, Prog. Theor. Phys. **13**, 119 (1955).